Available online at www.sciencedirect.com
SCIENCE DIRECT®
Journal of Sound and Vibration 282 (2005) 1137–1153
JOURNAL OF SOUND AND VIBRATION
www.elsevier.com/locate/jsvi

Thermal postbuckled vibrations of symmetrically laminated composite plates with initial geometric imperfections

J. Girish, L.S. Ramachandra*

Department of Civil Engineering, Indian Institute of Technology, Kharagpur 721302, India

Received 5 September 2003; accepted 25 March 2004

Abstract

In the present paper the postbuckling and postbuckled vibrations of symmetrically laminated composite plate subjected to a uniform temperature distribution through the thickness is presented. The structural model is based on a higher-order shear deformation theory incorporating von Kármán nonlinear strain–displacement relations and initial geometric imperfections. Adopting a multi-term Galerkin's approximation, the governing nonlinear partial differential equations are converted into a set of nonlinear algebraic equations in the case of postbuckling analysis and nonlinear ordinary differential equations in the case of free vibration analysis. The critical buckling temperatures are obtained from the solution of the corresponding linear eigenvalue problems. Postbuckled equilibrium paths are traced by solving the nonlinear algebraic equations, via the Newton–Raphson iterative procedure. The free vibration frequencies of a thermally postbuckled plate are reported by solving the eigenvalue problem for different postbuckled deflections.

1. Introduction

The problem of postbuckling of composite plates under thermal effect was investigated in the past using Rayleigh–Ritz [1], Galerkin [2–4], perturbation [5] and finite element methods [6–8]. However, relatively less work has been done in the area of free vibration analysis of thermally

*Corresponding author. Tel.: +91-3222-83444; fax: +91-3222-55303.
E-mail address: lsr@civil.iitkgp.ernet.in (L.S. Ramachandra).

0022-460X/$ - see front matter © 2004 Elsevier Ltd. All rights reserved.
doi:10.1016/j.jsv.2004.04.005

postbuckled-laminated composite plates. Bisplingoff and Pian [9] studied the small-amplitude vibration of a buckled isotropic rectangular plate with an aspect ratio of 3, subjected to a in-plane compression due to temperature loading. Yamaki [10] investigated the large-amplitude flexural vibrations of elastic plates, using one-term approximation of Galerkin's method. The influence of large amplitudes on free flexural vibrations of elastic plates was studied by Chu and Herrmann [11] using the perturbation method. Yang and Han [12] studied the buckled plate vibrations and large-amplitude vibrations using high-order triangular elements. Hui and Leissa [13] reported the effects of geometric imperfections on the vibration frequencies of simply supported flat plates under in-plane uniaxial or biaxial compression. Authors have used a single-term Galerkin's method to solve the nonlinear von Kármán's equation and numerical results are presented for isotropic, homogeneous plate. Illanko [14] studied the vibration and postbuckling of mechanically loaded rectangular plates using a multi-term Galerkin's procedure. Lee and Lee [15] reported the vibration behavior of thermally postbuckled anisotropic plates within the framework of finite element method. The finite element model is based on a first-order shear deformable plate theory considering von Kármán strain–displacement relation. Librescu et al. [16,17] studied the vibration behavior of geometrically imperfect flat and curved panels subjected to thermal and mechanical loads. The effects of tangential edge constraints on the vibrational behavior of single/multilayered doubly curved shallow panels subjected to complex thermomechanical loading are presented by Librescu and Lin [18]. In Refs. [16–18] the formulation is based on a higher-order shallow-shell theory and the governing equations of the problem were solved using a one-term Galerkin approximation. Ribeiro and Petyt [19] studied the nonlinear vibration of composite-laminated plates by the hierarchical finite element and the harmonic balance methods. Free and steady-state forced vibrations were analyzed considering three harmonics. Oh et al. [20] studied the postbuckling and vibration characteristics of piezolaminated composite plates, using nonlinear finite element equations based on the layerwise displacement theory. In a companion paper, Oh and Lee [21] investigated thermal snapping and vibration characteristics of cylindrical composite panels using the layerwise theory. Recently, Liew et al. [22] investigated the postbuckling of piezoelectric FGM plates subject to thermo-electro-mechanical loading. Yang et al. [23] reported the large-amplitude vibration analysis of FGM-laminated plates, subject to thermo-electro-mechanical loading.

While reviewing the preceding developments, it is observed that the existing formulations do not cover the free vibration analysis of thermally postbuckled imperfect composite plates considering higher-order shear deformation theory. Hence, the present study is focused on postbuckling and postbuckled vibration analysis of symmetrically laminated composite plates subjected to uniform temperature distribution through the thickness, using a multi-term Galerkin procedure. The multi-term approach is essential because of the fact that, the postbuckling deflection is the combination of different modes. The formulation is based on a higher-order shear deformation plate theory, incorporating von Kármán nonlinear strain-displacement relations. The displacement field used in the present study corresponds to the higher-order shear deformation theory proposed by Reddy [24]. Reddy has used principle of virtual displacements to derive the equilibrium equations appropriate to the assumed displacement fields. However, in the present approach, the equations of equilibrium are obtained using the principle of minimum total potential energy. The boundary conditions at all edges are assumed to be simply supported and immovable. Numerical results are presented for eight-layered symmetric crossply $(0/90/90/0)_s$

graphite epoxy laminates including initial geometric imperfections. Adopting Galerkin procedure, the governing nonlinear partial differential equations are converted into a set of nonlinear algebraic equations in the case of postbuckling analysis and nonlinear ordinary differential equations in the case of free vibration analysis. The nonlinear algebraic equations are solved using the Newton–Raphson iterative procedure. The free vibration frequencies of a thermally postbuckled plate are obtained by solving the eigenvalue problem for different postbuckled deflections.

2. Formulation

Consider a plate of constant thickness h composed of a finite number of orthotropic layers. The coordinate system is such that the middle plane of the plate coincides with the x–y plane, and the z-axis is normal to the middle plane. The higher-order shear deformation theory used in the present study is based on the following displacement field given by Reddy [24] and are expressed as

$$u = u^0 - zw^0_{,x} + f(z)\phi_1; \quad v = v^0 - zw^0_{,y} + f(z)\phi_2; \quad w = w^0, \tag{1}$$

where

$$\phi_1 = \varphi_1 + w^0_{,x}, \quad \phi_2 = \varphi_2 + w^0_{,y}, \quad f(z) = z\left[1 - \frac{4}{3}\left(\frac{z}{h}\right)^2\right].$$

Here u, v, w are displacement components, respectively, along x, y, z directions; u^0, v^0, w^0 are the displacements of a generic point in the mid-plane; and φ_1 and φ_2 are the rotations of the cross-sections perpendicular to the x- and y-axis, respectively. The governing equations of the problem under investigation are the equations of motion of the plate, the constitutive law and the strain–displacement equations. By neglecting in-plane inertia terms, the equations of equilibrium can be obtained using the principle of minimum total potential energy as

$$\begin{aligned}
&N_{x,x} + N_{xy,y} = 0,\\
&N_{xy,x} + N_{y,y} = 0,\\
&M_{x,xx} + 2M_{xy,xy} + M_{y,yy} + N_x w_{,xx} + 2N_{xy} w_{,xy} + N_y w_{,yy} = \rho w^0_{,tt},\\
&Q_{x,x} + Q_{xy,y} - V_{xz} = 0,\\
&Q_{yx,x} + Q_{y,y} - V_{yz} = 0,
\end{aligned} \tag{2}$$

where $(\,)_{,x}$ denotes partial differentiation with respect to x. N_x, N_y, N_{xy}, Q_x, Q_y, Q_{xy}, V_{xz}, V_{yz} and M_x, M_y, M_{xy} are the stress and moment resultants, which are given by

$$\left(\begin{pmatrix} N_x \\ N_y \\ N_{xy} \end{pmatrix}, \begin{pmatrix} M_x \\ M_y \\ M_{xy} \end{pmatrix}, \begin{pmatrix} Q_x \\ Q_y \\ Q_{xy} \end{pmatrix}\right) = \int_{-h/2}^{h/2} \begin{pmatrix} \sigma_x \\ \sigma_y \\ \tau_{xy} \end{pmatrix} (1,\ z,\ f(z))\,\mathrm{d}z, \tag{3}$$

$$(V_{xz}, V_{yz}) = \int_{-h/2}^{h/2} (\tau_{xz}, \tau_{yz}) f'(z)\,\mathrm{d}z$$

where $f'(z) = (\mathrm{d}/\mathrm{d}z)f(z)$.

The stresses are related to strains as

$$\{\sigma\} = [\overline{Q}](\{\varepsilon\} - \{\alpha\}T) \tag{4}$$

where

$$\{\sigma\}^{\mathrm{T}} = \{\sigma_x \ \ \sigma_y \ \ \tau_{xy} \ \ \tau_{yz} \ \ \tau_{xz}\},$$
$$\{\varepsilon\}^{\mathrm{T}} = \{\varepsilon_x \ \ \varepsilon_y \ \ \gamma_{xy} \ \ \gamma_{yz} \ \ \gamma_{xz}\},$$
$$\{\alpha\}^{\mathrm{T}} = \{\alpha_{xx} \ \ \alpha_{yy} \ \ \alpha_{xy}\},$$

where $[\overline{Q}]$ are the transformed in-plane reduced stiffnesses. $\{\sigma\}^{\mathrm{T}}$are the Cartesian components of stress tensor at any point, $\{\varepsilon\}^{\mathrm{T}}$ are the corresponding strain tensor and $\{\alpha\}^{\mathrm{T}}$ are linear thermal expansion coefficients. The strain components at a distance 'z' away from the mid-plane are related to mid-surface strains of a perfect flat plate as follows:

$$\begin{aligned}
\varepsilon_x &= \varepsilon_x^0 - zw_{,xx}^0 + f(z)\phi_{1,x},\\
\varepsilon_y &= \varepsilon_y^0 - zw_{,yy}^0 + f(z)\phi_{2,y},\\
\gamma_{xy} &= \varepsilon_{xy}^0 - 2zw_{,xy}^0 + f(z)\phi_{1,y} + f(z)\phi_{2,x},\\
\gamma_{xz} &= u_{,z} + w_{,x} = f'(z)\phi_1,\\
\gamma_{yz} &= v_{,z} + w_{,y} = f'(z)\phi_2,
\end{aligned} \tag{5}$$

$\varepsilon_x^0, \varepsilon_y^0$ and γ_{xy}^0 are reference surface strains and are defined as

$$\begin{aligned}
\varepsilon_x^0 &= u_{,x}^0 + \tfrac{1}{2}(w_{,x}^0)^2,\\
\varepsilon_y^0 &= v_{,y}^0 + \tfrac{1}{2}(w_{,y}^0)^2,\\
\gamma_{xy}^0 &= u_{,y}^0 + v_{,x}^0 + w_{,x}^0 w_{,y}^0.
\end{aligned} \tag{6}$$

The geometric imperfection of a plate is assumed as

$$w^* = w_0 \sin\frac{m\pi x}{a} \sin\frac{n\pi y}{b}, \tag{7}$$

where m, n are half-wave numbers. Moreover, a, b are the plate dimensions along x and y directions respectively. The coefficient w_0 represents the value of initial imperfection at the plate center. The strains due to initial imperfection at the mid surface can be written as [25]

$$\varepsilon_x^* = \tfrac{1}{2}(w_{,x}^*)^2; \quad \varepsilon_y^* = \tfrac{1}{2}(w_{,y}^*)^2; \quad \gamma_{xy}^* = w_{,x}^* w_{,y}^*; \quad \gamma_{xz}^* = w_{,x}^*; \quad \gamma_{yz}^* = w_{,y}^*. \tag{8}$$

Thus, the net strain components of the imperfect plate are

$$\begin{aligned}
\varepsilon_x &= \varepsilon_x^0 + w_{,x}^0 w_{,x}^* - zw_{,xx}^0 + f(z)\phi_{1,x},\\
\varepsilon_y &= \varepsilon_y^0 + w_{,y}^0 w_{,y}^* - zw_{,yy}^0 + f(z)\phi_{2,y},\\
\gamma_{xy} &= \gamma_{xy}^0 + w_{,x}^0 w_{,y}^* + w_{,x}^* w_{,y}^0 - 2zw_{,xy}^0 + f(z)\phi_{1,y} + f(z)\phi_{2,x},\\
\gamma_{xz} &= u_{,z} + w_{,x} = f'(z)\phi_1,\\
\gamma_{yz} &= v_{,z} + w_{,y} = f'(z)\phi_2.
\end{aligned} \tag{9}$$

By expressing the stress resultants in terms of displacements in Eq. (2), the governing equations of motion in unknown displacements are obtained and are given in Appendix A.

3. Solution procedure

Consider a rectangular plate of length a, width b and thickness h. Simply supported immovable edge boundary conditions are considered on all four sides of the plate and are stated as

$$u^0 = v^0 = w^0 = 0 \quad \text{at } x = 0,\ a \text{ and } y = 0, b. \tag{10}$$

The Galerkin procedure is adopted to solve the governing partial differential equations (A.1)–(A.5), wherein the displacement fields are represented as

$$\begin{aligned}
u^0 &= \sum_{i=1}^{m}\sum_{j=1}^{n} U_{ij} \sin\left(\frac{2i\pi x}{a}\right) \sin\left(\frac{j\pi y}{b}\right); \quad \phi_1 = \sum_{i=1}^{m}\sum_{j=1}^{n} \alpha_{ij} \sin\left(\frac{2i\pi x}{a}\right) \sin\left(\frac{j\pi y}{b}\right),\\
v^0 &= \sum_{i=1}^{m}\sum_{j=1}^{n} V_{ij} \sin\left(\frac{i\pi x}{a}\right) \sin\left(\frac{2j\pi y}{b}\right); \quad \phi_2 = \sum_{i=1}^{m}\sum_{j=1}^{n} \beta_{ij} \sin\left(\frac{i\pi x}{a}\right) \sin\left(\frac{2j\pi y}{b}\right),\\
w^0 &= \sum_{i=1}^{m}\sum_{j=1}^{n} W_{ij} \sin\left(\frac{i\pi x}{a}\right) \sin\left(\frac{j\pi y}{b}\right).
\end{aligned} \tag{11}$$

Neglecting inertia term in equations (A.1)–(A.5) and applying Galerkin procedure, one obtains a system of nonlinear algebraic equations in constant coefficients U_{ij}, V_{ij}, W_{ij}, α_{ij} and β_{ij}. For one-term ($m = n = 1$) Galerkin approximation, the five nonlinear-coupled algebraic equations are

$$\begin{gathered}
R_1 U_{11} + R_2 V_{11} + R_3 W_{11}^2 = 0,\\
R_4 U_{11} + R_5 V_{11} + R_6 W_{11}^2 = 0,\\
R_7 U_{11} W_{11} + R_8 V_{11} W_{11} + R_9 W_{11} + R_{10} W_{11}^3 + R_{11}\lambda T_{cr} W_{11} + R_{12}\alpha_{11} + R_{13}\beta_{11} = 0,\\
R_{14} W_{11} + R_{15}\alpha_{11} + R_{16}\beta_{11} = 0,\\
R_{17} W_{11} + R_{18}\alpha_{11} + R_{19}\beta_{11} = 0,
\end{gathered} \tag{12}$$

where λ is the load factor and T_{cr} is the critical buckling temperature of the plate.

Using the Newton–Raphson method, the system of nonlinear algebraic equations can be solved and the postbuckled deflections obtained. The constants of integration R_1 to R_{19} are given in Appendix B. The nonlinear algebraic equations based on a multi-term Galerkin procedure are not presented for the sake of brevity.

3.1. Small-amplitude vibration about a static equilibrium state

For the free vibration analysis of plates about a prebuckling and postbuckling equilibrium states, the unknown modal amplitudes are assumed to be the sum of time-independent and time-dependent solution, which may be written as

$$\{w\} = \{w_s\} + \{w_t\}, \tag{13}$$

where $\{w_s\}$ is the thermal postbuckling deflection and w_t is the small vibration amplitude about a static equilibrium state. In the case of small-amplitude vibration $\{w_t\}^2 \ll \{w_s\}$. Substituting the displacement field (Eq. (11)) into the governing partial differential equations (A.1)–(A.5) and adopting the Galerkin's technique, we can obtain a set of nonlinear ordinary differential equations. For the free vibration analysis at frequency 'ω', the following one-harmonic approximation is assumed to solve the ordinary differential equations:

$$W_{ij}(t) = \tilde{W}_{ij} \sin \omega t. \tag{14}$$

Using the above function the nonlinear ordinary differential equations are converted into a set of nonlinear algebraic equations. In the analysis, the in-plane inertia terms are neglected and consequently the in-plane displacements become a function of $\sin^2 \omega t$. Now condensing the equations of motion, the standard eigenvalue problem is obtained [15,16–18]. For the linear vibration analysis about a static equilibrium state, the nonlinear algebraic equations can be arranged into the following eigenvalue equation:

$$\{([K] - \lambda T_{cr}[K_{\Delta T}] + [N]) - \omega^2[M]\}\{w_t\} = 0, \tag{15}$$

where $[K]$ and $[K_{\Delta T}]$ are linear elastic stiffness and linear stiffness due to thermal load; $[N]$ is the nonlinear stiffness due to large deformation; $[M]$ is the mass matrix. In Eq. (15), the nonlinear stiffness matrix $[N]$ is a function of only time-independent amplitude. By substituting the converged postbuckling deflection values obtained from the postbuckling analysis, the vibration analysis is performed by solving eigenvalue equation (15).

3.2. Large-amplitude vibration about a static equilibrium state

For the large-amplitude vibration analysis, the in-plane inertia terms may still be neglected. It may be pointed out that, for the large-amplitude vibration about a postbuckled equilibrium state, the one-term harmonic (Eq. (14)) assumption is an approximation. Using the one-term harmonic function (Eq. (14)), the nonlinear ordinary differential equations can be converted into a set of nonlinear algebraic equations. The equations can be arranged into the following eigenvalue equation:

$$\{([K] - \lambda T_{cr}[K_{\Delta T}] + [K_N]) - \omega^2[M]\}\{w\} = 0, \tag{16}$$

where $[K_N]$ is a nonlinear stiffness matrix, which is a function of sum of time-dependent and time-independent (postbuckled deflections) amplitudes. Hence, the nonlinear eigenvalue problem given by Eq. (16) is solved by iterative procedure (for more details see Ref. [26]).

4. Numerical results and discussion

Numerical results are presented for eight-layered symmetric crossply $(0/90/90/0)_s$ graphite epoxy laminate subjected to a uniform temperature distribution through the thickness. The

graphite epoxy material properties are taken as [27]:

$$E_1 = 155\,\text{GPa}; \quad E_2 = 8.07\,\text{GPa}; \quad \mu_{12} = 0.22,$$
$$G_{12} = 4.55\,\text{GPa}; \quad G_{23} = 3.25\,\text{GPa}; \quad \rho = 1586\,\text{Kg/m}^3,$$
$$\alpha_1 = -0.07 \times 10^{-6}/^\circ\text{C}; \quad \alpha_2 = 30.1 \times 10^{-6}/^\circ\text{C},$$

To validate the present formulation, the critical buckling temperature obtained from the present analysis for the symmetric crossply $(0/90/90/0)_s$, graphite epoxy laminate has been compared with that of Shi et al. [27]. The critical buckling temperature T_{cr} of the plate ($a/b = 1.25$) subjected to a uniform temperature distribution through the thickness in the reference is 6.8 °C and that in the present analysis is 6.8 °C. Next, thermal postbuckling equilibrium path is obtained using one-term Galerkin's approach and is compared with Shi et al. [27] in Fig. 1. It is observed from the figure that the results compare well.

Fig. 2 shows the response of nondimensionalized critical temperature (T^*) versus side-to-thickness ratio (a/h) of a square crossply $(0/90/90/0)_s$ laminate, obtained from the classical plate theory (CPT) and the higher-order shear deformation (HSDT) theory. It can be seen that, if the plate a/h is $\geqslant 50$, both the theories predicts the same results. However, if side-to-thickness ratio of plate a/h is < 50, the classical plate theory overpredicts the buckling load. Hence, it is necessary to consider the shear deformation theory, when a/h is less than 50.

Nonlinear equilibrium paths of a thin ($a/h = 250$) eight-layered symmetric crossply, simply supported, square ($a/b = 1$) and rectangular ($a/b = 3$) plates are shown in Figs. 3 and 4 respectively. At lower temperature the 1-mode ($m = n = 1$) Galerkin approximation predicts accurate postbuckling deflection of the plate. However, at higher temperatures more modes are required to predict the postbuckled shape of the plate. At a postbuckled temperature $T = 10T_{cr}$, for a rectangular plate with aspect ratio of 3, the difference between the 1-term ($m = n = 1$) and 4-term ($m = n = 1,3$) solutions is 52.8%, whereas the difference between 3-term ($mn = 11,13,31$) and

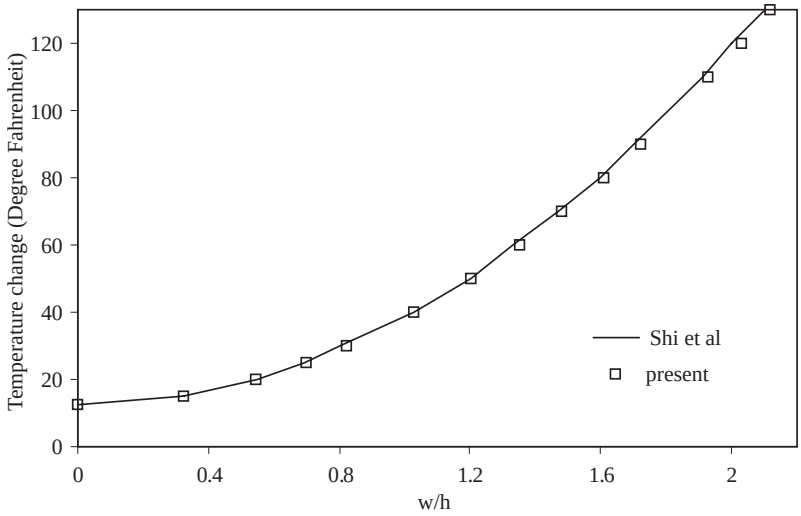

Fig. 1. Postbuckled deflection path for a rectangular laminated plate ($a/b = 1.25$, $(0/90/90/0)_s$).

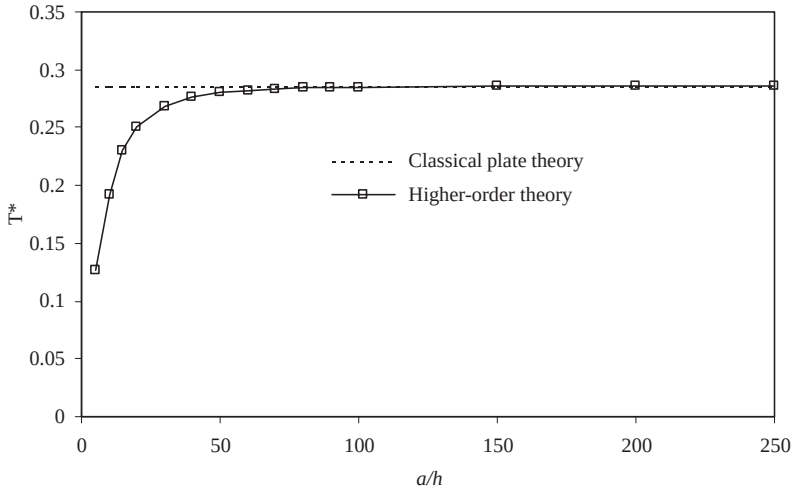

Fig. 2. Nondimensionalized critical temperature versus side-to-thickness ratio of a square laminated plate ($T^* = T_{cr}a^2h\alpha_2/\pi^2D_{22}$, $a/b = 1$, $(0/90/90/0)_s$).

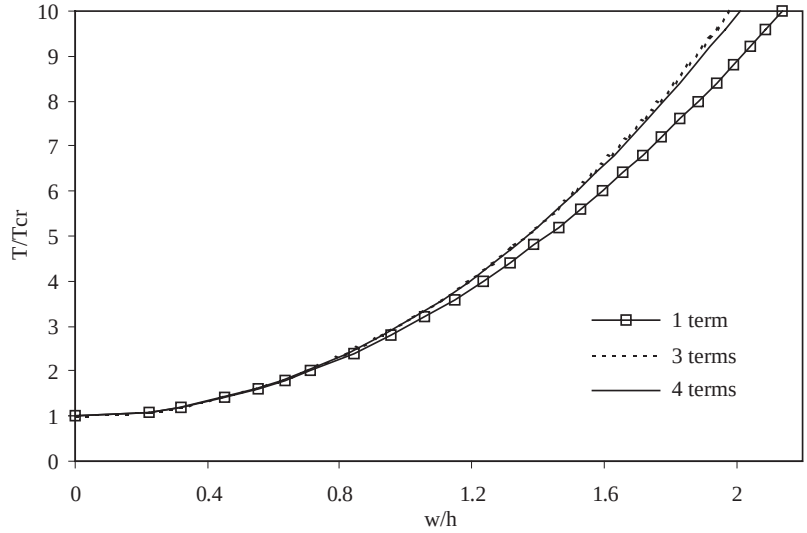

Fig. 3. Postbuckled deflection paths for a square laminated plate ($a/b = 1.0$, $(0/90/90/0)_s$).

4-term solutions is less than 1%. Thus, three terms are sufficient to obtain accurate results for the problems considered in this paper.

Tables 1 and 2 show the contribution of each mode of the assumed displacement function (Eq. (11)), to the central deflections of plates for the aspect ratios (a/b) of 1 and 3, respectively, at various temperatures. It may be seen that the participation of the first mode (w_{11}) postbuckled deflection decreases as the temperature increases, whereas the contributions of other three modes (w_{13}, w_{31}, w_{33}) increase. Hence, at high temperatures a 1-term approach will not give accurate postbuckling deflection and multi-terms need to be used in the displacement function of

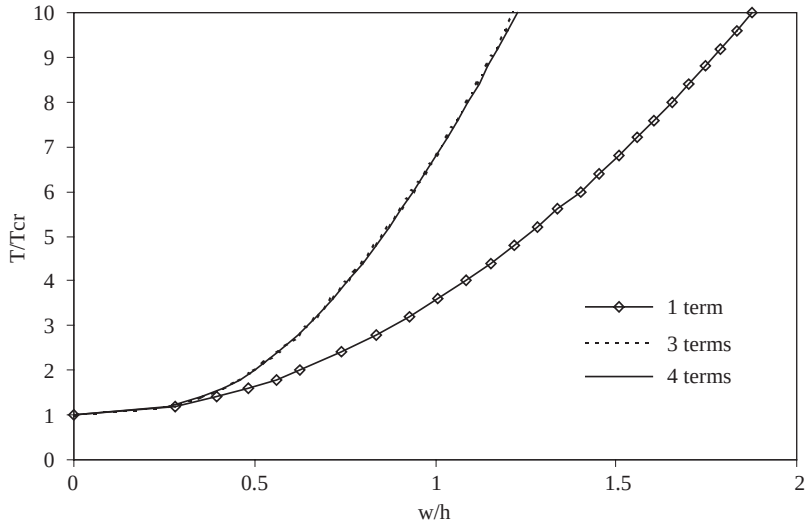

Fig. 4. Postbuckled deflection paths for a rectangular laminated plate ($a/b=3$, $(0/90/90/0)_s$).

Table 1
Modal participation values (%) $a/b=1$

T/T_{cr}	w_{11}	w_{13}	w_{31}	w_{33}
4	96.37	2.08	1.38	0.16
8	89.77	5.44	3.53	1.26
12	82.76	8.26	5.97	3.00
16	79.14	9.45	7.57	3.83
20	77.43	9.95	8.46	4.17

Table 2
Modal participation values (%) $a/b=3$

T/T_{cr}	w_{11}	w_{13}	w_{31}	w_{33}
2	79.79	0.006	20.20	0.007
4	74.32	0.03	25.58	0.072
8	72.00	0.13	27.55	0.288
12	70.84	0.39	28.03	0.73
16	69.40	1.19	27.57	1.84
20	68.60	2.00	26.16	3.24

Galerkin's approximation. This is more so when the plate is rectangular. Fig. 5(a) shows the postbuckled deflection contour of a rectangular plate ($a/b=3$) at a temperature $T=3.0T_{cr}$ for the one-term Galerkin approximation. The results of the four-term Galerkin approximation are shown in Fig. 5(b). The four-term deflection contour is quite different from that of the one-term contour. The one-term deflection contour shape remains the same through out the postbuckling

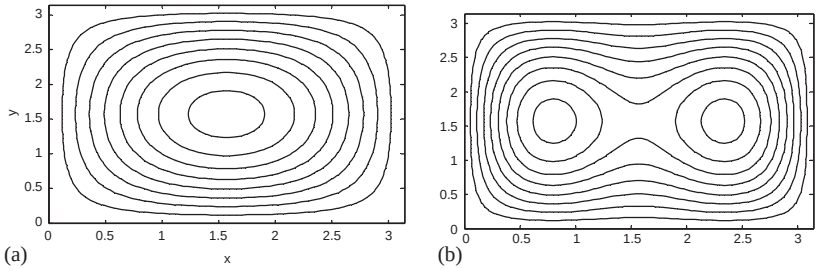

Fig. 5. Postbuckled deflection contours for a rectangular laminated plate ($T/T_{cr}=3$, $a/b=3$, $(0/90/90/0)_s$): (a) one-term deflection contour, (b) four-term deflection contour.

range as it has only one term in the formulation. Hence, a multi-term solution is essential in order to obtain the true postbuckled deflected shape of the plate. The participation of each term/mode in the total deflection is calculated as [27]

$$\text{Participation of } i\text{th mode in the total deflection} = |w_i| \Big/ \sum_{j=1}^{N} |w_j|, \tag{17}$$

where w_i is the deflection due to ith mode and N is the number of modes considered in the displacement function (Eq. (11)).

Fig. 6 shows the thermal postbuckling equilibrium paths for three different aspect ratios of a plate $a/b=1$, 2 and 3. The curves are shown for perfect plate (w_0=0) and also with an initial geometric imperfection of 0.1 times the thickness (h) of the plate. The length of the plate a is kept constant and $a/h=250$. That is, the higher the value of a/b becomes, the lower the width of the plate b becomes. The temperatures have been normalized by T^*_{cr}, the buckling temperature of a square laminate. As the aspect ratio of the plate increases, the slope of the curves increases, thereby indicating higher postbuckling strength. Due to the presence of the initial imperfections, bifurcation buckling does not take place. The plate starts deflecting as soon as the temperature is increased.

The effect of transverse shear–deformation on the response of nondimensionalized fundamental frequency (ω*) versus temperature load (T*), for various plate side-to-thickness ($a/h=10$, 25, 50, 250) ratios of a square laminate is shown in Fig. 7. It can be seen that, as the plate side-to-thickness ratio increases, the fundamental frequency decreases in the prebuckling and postbuckling region, whereas the critical temperature increases.

Figs. 8–10 show response of the vibration frequency ω/ω_0 versus temperature ratio T/T^*_{cr}, for the aspect ratios of the plate 1, 2 and 3 respectively. In the figures, modes 1, 2 and 3 correspond to different half-waves along $\bar{x}$ and y- directions viz; $m=n=1$ (mode 1); $m=1$, $n=3$ (mode 2); $m=3$, $n=1$ (mode 3). The frequencies have been normalized by the lowest linear natural frequency ω_0 of the plate. Zero frequency (mode 1) corresponds to critical buckling temperature. The frequency of the pre- and postbuckled plates in all the three modes increases with the increase in temperature, due to the increase in nonlinear stiffness. From these curves it may be observed that the presence of a small imperfection of the plate has pronounced effect on the vibration frequencies.

The response of large-amplitude variation versus frequency has been shown in Fig. 11. The amplitude is normalized with the thickness of the plate, whereas the frequency has been

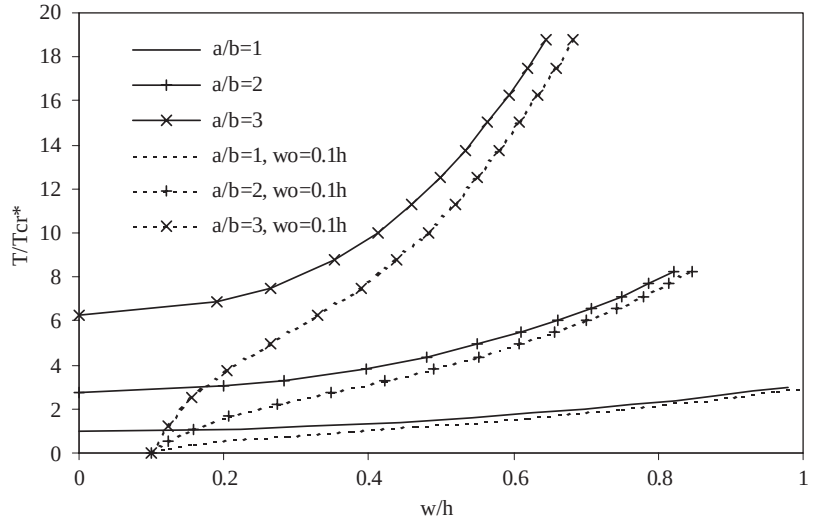

Fig. 6. Postbuckled deflection curves for different aspect ratios (a/b) of the laminated plate $(0/90/90/0)_s$.

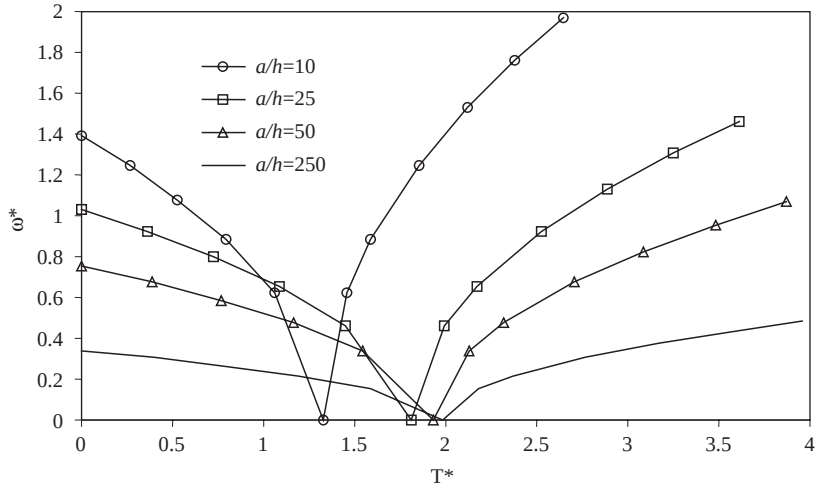

Fig. 7. Effects of transverse shear–deformation on the response of fundamental frequency versus temperature load of a square laminated plate. ($\omega* = \omega a^2/h\sqrt{\rho/E_2}$, $T* = T_{cr}a^2h\alpha_2/\pi^2D_{22}$, $a/b = 1$, $(0/90/90/0)_s$).

normalized with the natural frequency ω_0 of the plate. The results were shown for $T/T_{cr}=0$, 1, and 2, respectively. In the figure, the curve for temperature load $T/T_{cr}=0$ corresponds to a large-amplitude free vibration analysis, without a temperature load. Similarly, the curve for $T/T_{cr}=1$, corresponds to bifurcation buckling of a plate, the determinant of the sum of the elastic linear stiffness matrix and stiffness matrix due to thermal load vanishes. As a result, the amplitude-frequency curve appears to be linear. The curve $T/T_{cr}=2$, represents a large-amplitude free vibration, about a postbuckled equilibrium state.

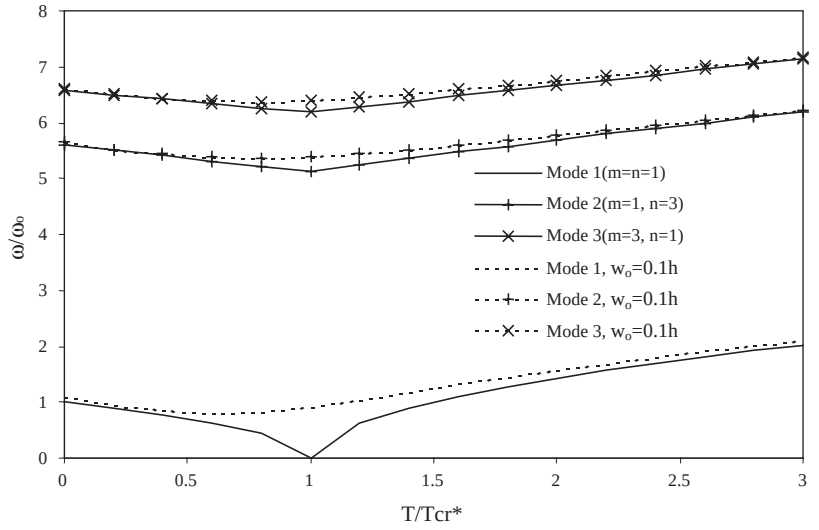

Fig. 8. Natural frequencies of the pre- and postbuckled square laminated plate ($a/b = 1.0$, $(0/90/90/0)_s$).

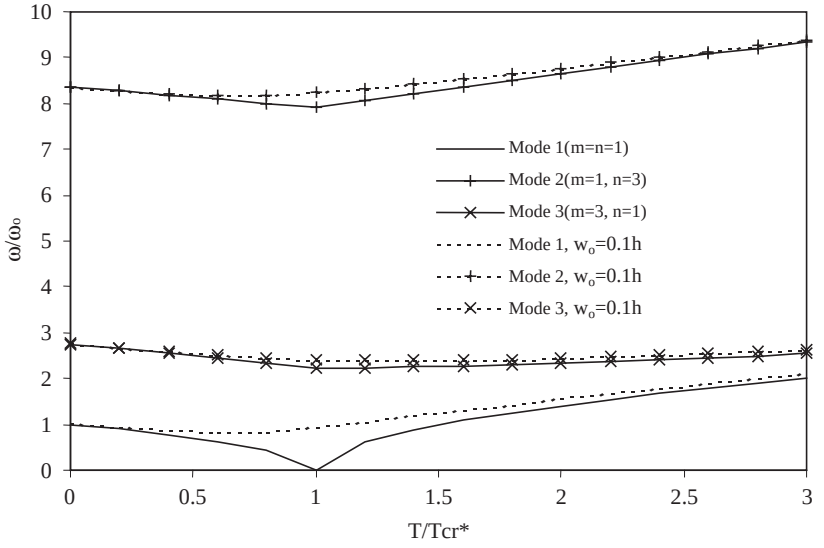

Fig. 9. Natural frequencies of the pre- and postbuckled rectangular laminated plate ($a/b = 2.0$, $(0/90/90/0)_s$).

5. Concluding remarks

A formulation based on higher-order shear deformation plate theory, including von Kármán strain–displacement relation and initial geometric imperfection is presented for solving thermal

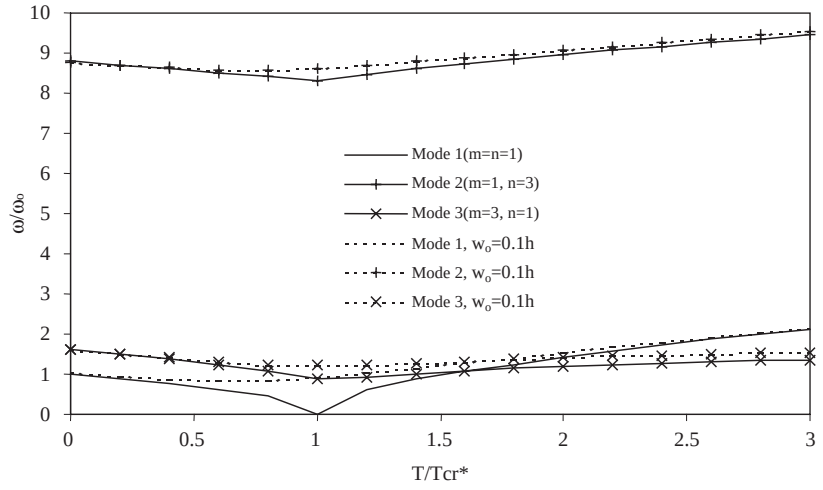

Fig. 10. Natural frequencies of the pre- and postbuckled rectangular laminated plate ($a/b = 3.0$, $(0/90/90/0)_s$).

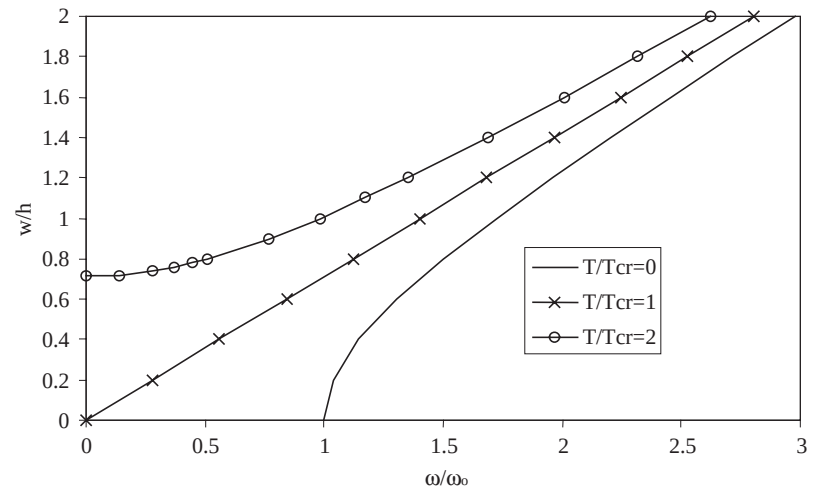

Fig. 11. First mode, amplitudes versus frequencies of a square laminated plate ($a/b = 1.0$, $(0/90/90/0)_s$).

postbuckling and postbuckled vibrations of symmetric crossply laminated composite plates. Multi-term Galerkin method is implemented to obtain the true postbuckled shape of the plate and higher mode vibration frequencies. The effect of aspect ratio on the critical buckling temperature and postbuckling response is significant. From the present study, it is observed that the multimode Galerkin method gives better results than the single mode solution. This is more so in the case of rectangular plate. The influence of initial geometric imperfection on the postbuckling path has

been studied. It is seen from the present study that, as the side-to-thickness ratio of plate increases, the fundamental frequency decreases in the pre- and postbuckling region, whereas the critical temperature increases. Free vibration characteristics of a pre- and postbuckled plate, with and without initial geometric imperfections were investigated, for the different aspect ratios of the plate. It is observed that the initial geometric imperfection has significant influence on the frequencies.

Acknowledgements

The authors wish to acknowledge the Aeronautics Research and Development Board (AR&DB), India, for their financial support.

Appendix A

$$\begin{aligned} &A_{11}u^0_{,xx} + A_{66}u^0_{,yy} + (A_{12}+A_{66})v^0_{,xy} + \{A_{11}(w^0_{,xx} + w^*_{,xx}) \\ &\quad + A_{66}(w^0_{,yy} + w^*_{,yy})\}w^0_{,x} + (A_{11}w^0_{,xx} + A_{66}w^0_{,yy})w^*_{,x} \\ &\quad + (A_{12}+A_{66})(w^0_{,y}w^0_{,xy} + w^0_{,y}w^*_{,xy} + w^*_{,y}w^0_{,xy}) = 0, \end{aligned} \tag{A.1}$$

$$\begin{aligned} &(A_{12}+A_{66})u^0_{,xy} + A_{66}v^0_{,xx} + A_{22}v^0_{,yy} + \{A_{66}(w^0_{,xx} + w^*_{,xx}) \\ &\quad + A_{22}(w^0_{,yy} + w^*_{,yy})\}w^0_{,y} + (A_{66}w^0_{,xx} + A_{22}w^0_{,yy})w^*_{,y} \\ &\quad + (A_{12}+A_{66})(w^0_{,x}w^0_{,xy} + w^0_{,x}w^*_{,xy} + w^*_{,x}w^0_{,xy}) = 0, \end{aligned} \tag{A.2}$$

$$\begin{aligned} &-\{C_{11}w^0_{,xxxx} + 2(C_{12}+2C_{66})w^0_{,xxyy} + C_{22}w^0_{,yyyy}\} + E_{11}\phi_{1,xxx} \\ &\quad + (E_{12}+2E_{66})(\phi_{1,xyy} + \phi_{2,xxy}) + E_{22}\phi_{2,yyy} \\ &\quad + [A_{11}\{u^0_{,x} + \tfrac{1}{2}(w^0_{,x})^2 + w^0_{,x}w^*_{,x}\} + A_{12}\{v^0_{,y} + \tfrac{1}{2}(w^0_{,y})^2 + w^0_{,y}w^*_{,y}\} - N^T_x](w^0 + w^*)_{,xx} \\ &\quad + 2\{A_{66}(u^0_{,y} + v^0_{,x} + w^0_{,x}w^0_{,y} + w^0_{,x}w^*_{,y} + w^*_{,x}w^0_{,y}) - N^T_{xy}\}(w^0 + w^*)_{,xy} \\ &\quad + [A_{12}\{u^0_{,x} + \tfrac{1}{2}(w^0_{,x})^2 + w^0_{,x}w^*_{,x}\} + A_{22}\{v^0_{,y} + \tfrac{1}{2}(w^0_{,y})^2 + w^0_{,y}w^*_{,y}\} - N^T_y](w^0 + w^*)_{,yy} = \rho w^0_{,tt}, \end{aligned} \tag{A.3}$$

$$-E_{11}w^0_{,xxx} - (E_{12}+2E_{66})w^0_{,xyy} + F_{11}\phi_{1,xx} + F_{66}\phi_{1,yy} + (F_{12}+F_{66})\phi_{2,xy} - H_{55}\phi_1 = 0, \tag{A.4}$$

$$-E_{22}w^0_{,yyy} - (E_{12}+2E_{66})w^0_{,xxy} + F_{66}\phi_{2,xx} + F_{22}\phi_{2,yy} + (F_{12}+F_{66})\phi_{1,xy} - H_{44}\phi_2 = 0, \tag{A.5}$$

where $(A_{ij}, C_{ij}) = \int_{-h/2}^{h/2} Q_{ij}(1, z^2)\,\mathrm{d}z$; $(E_{ij}, F_{ij}) = \int_{-h/2}^{h/2} Q_{ij}(z, f(z))f(z)\,\mathrm{d}z$ for $i, j = 1, 2, 6$.

Appendix B

$$
\begin{aligned}
R_1 &= -\frac{\pi^2}{a^2}\left[4A_{11} + \left(\frac{a}{b}\right)^2 A_{66}\right],\\
R_2 &= -\frac{64}{9ab}[A_{12} + A_{66}],\\
R_3 &= -\frac{4\pi^2}{3a^3}\left[A_{11} - \frac{1}{2}\left(\frac{a}{b}\right)^2 (A_{12} - A_{66})\right],\\
R_4 &= -\frac{64}{9ab}[A_{12} + A_{66}],\\
R_5 &= -\frac{\pi^2}{a^2}\left[4\left(\frac{a}{b}\right)^2 A_{22} + A_{66}\right],\\
R_6 &= -\frac{4\pi^2}{3a^3}\left[\left(\frac{a}{b}\right)^3 A_{22} - \frac{1}{2}\left(\frac{a}{b}\right)(A_{12} - A_{66})\right],\\
R_7 &= \frac{8\pi^2}{3a^3}\left[A_{11} + \left(\frac{a}{b}\right)^2 A_{12} + \frac{1}{2}\left(\frac{a}{b}\right)^2 A_{66}\right],\\
R_8 &= \frac{8\pi^2}{3a^3}\left[\left(\frac{a}{b}\right)^3 A_{22} + \left(\frac{a}{b}\right) A_{12} + \frac{1}{2}\left(\frac{a}{b}\right) A_{66}\right],\\
R_9 &= -\frac{\pi^4}{a^4}\left[C_{11} + 2\left(\frac{a}{b}\right)^2 (C_{12} + 2C_{66}) + \left(\frac{a}{b}\right)^4 C_{22}\right],\\
R_{10} &= -\frac{\pi^4}{32a^4}\left[3A_{11} + 6\left(\frac{a}{b}\right)^2 A_{12} + 3\left(\frac{a}{b}\right)^4 A_{22} + 4\left(\frac{a}{b}\right)^2 A_{66}\right],\\
R_{11} &= \frac{\pi^2}{a^2}\left[N_x^T + \left(\frac{a}{b}\right)^2 N_y^T\right],\\
R_{12} &= \frac{8\pi^2}{3a^3}\left[4E_{11} + \left(\frac{a}{b}\right)^2 (E_{12} + 2E_{66})\right],\\
R_{13} &= \frac{8\pi^2}{3a^3}\left[4\left(\frac{a}{b}\right)^3 E_{22} + \left(\frac{a}{b}\right)(E_{12} + 2E_{66})\right],\\
R_{14} &= -\frac{8\pi^2}{3a^3}\left[E_{11} + \left(\frac{a}{b}\right)^2 (E_{12} + 2E_{66})\right],\\
R_{15} &= -\frac{\pi^2}{a^2}\left[4F_{11} + \left(\frac{a}{b}\right)^2 F_{66} + \left(\frac{a}{\pi}\right)^2 H_{55}\right],\\
R_{16} &= -\frac{64}{9ab}[F_{12} + F_{66}],\\
R_{17} &= -\frac{8\pi^2}{3a^3}\left[\left(\frac{a}{b}\right)^3 E_{22} + \left(\frac{a}{b}\right)(E_{12} + 2E_{66})\right],
\end{aligned}
$$

$$R_{18} = -\frac{64}{9ab}[F_{12} + F_{66}],$$

$$R_{19} = -\frac{\pi^2}{a^2}\left[4\left(\frac{a}{b}\right)^2 F_{22} + F_{66} + \left(\frac{a}{\pi}\right)^2 H_{44}\right].$$

References

[1] C.A. Meyers, M.W. Hyer, Thermal buckling and postbuckling of symmetrically laminated composite plates, *Journal of Thermal Stresses* 14 (1991) 519–540.

[2] L. Librescu, M.A. Souza, Post-buckling of geometrically imperfect shear-deformable flat panels under combined thermal and compressive edge loading, *Journal of Applied Mechanics* 60 (1993) 526–533.

[3] L. Librescu, W. Lin, M.P. Nemeth, J.H. Starnes, Thermomechanical postbuckling of geometrically imperfect flat and curved panels taking into account tangential constraints, *Journal of Thermal Stresses* 18 (1995) 465–482.

[4] L. Librescu, M.P. Nemeth, J.H. Starnes, W. Lin, Nonlinear response of flat and curved panels subjected to thermomechanical loads, *Journal of Thermal Stresses* 23 (2000) 549–582.

[5] H.S. Shen, Thermomechanical post-buckling analyses of imperfect laminated plates using a higher order shear-deformation theory, *Computers and Structures* 66 (1998) 395–409.

[6] L.W. Chen, L.Y. Chen, Thermal postbuckling behaviors of laminated composite plates with temperature dependent properties, *Composite Structures* 19 (1991) 267–283.

[7] G. Singh, G.V. Rao, N.G.R. Iyenger, Thermal postbuckling behavior of laminated composite plates, *AIAA Journal* 32 (1994) 1336–1338.

[8] M.K. Singha, L.S. Ramachandra, J.N. Bandyopadhyay, Thermal postbuckling analysis of laminated composite plates, *Composite Structures* 54 (2001) 453–458.

[9] R.L. Bisplinghoff, T.H.H. Pian, On the vibration of thermally buckled bars and plates, *Proceedings of the 9th International Congress for Applied Mechanics* 7 (1957) 307–318.

[10] N. Yamaki, Influence of large amplitude on flexural vibrations of elastic plates, *Zeitschrift für Angewandte Mathematik und Mechanik* 41 (1961) 501–510.

[11] H.N. Chu, G. Herrmann, Influence of large amplitudes on free flexural vibrations of rectangular elastic plates, *Journal of Applied Mechanics* 23 (1956) 532–540.

[12] T.Y. Yang, A.D. Han, Buckled plate vibrations and large amplitude vibrations using high-order triangular elements, *AIAA Journal* 21 (1983) 758–766.

[13] D. Hui, A.W. Leissa, Effects of geometric imperfections on vibrations of biaxially compressed rectangular flat plates, *Journal of Applied Mechanics* 50 (1983) 750–756.

[14] S. Illanko, Vibration and post-buckling of in-plane loaded rectangular plates using a multiterm Galerkin's method, *Journal of Applied Mechanics* 69 (2002) 589–592.

[15] D.M. Lee, I. Lee, Vibration behaviors of thermally postbuckled anisotropic plates using first-order shear deformable plate theory, *Computers and Structures* 63 (1997) 371–378.

[16] L. Librescu, W. Lin, M.P. Nemeth, J.H. Starnes, Vibration of geometrically imperfect panels subjected to thermal and mechanical loads, *Journal of Spacecraft and Rockets* 33 (1996) 285–291.

[17] L. Librescu, W. Lin, M.P. Nemeth, J.H. Starnes, Frequency–load interaction of geometrically imperfect curved panels subjected to heating, *AIAA Journal* 34 (1996) 166–177.

[18] L. Librescu, W. Lin, Vibration of thermomechanically loaded flat and curved panels taking into account geometric imperfections and tangential edge constraints, *International Journal of Solids Structures* 34 (1997) 2161–2181.

[19] P. Ribeiro, M. Petyt, Non-linear vibration of composite laminated plates by the hierarchical finite element method, *Composite Structures* 46 (1999) 197–208.

[20] I.K. Oh, J.H. Han, I. Lee, Postbuckling and vibration characteristics of piezolaminated composite plate subject to thermo-piezoelectric loads, *Journal of Sound and Vibration* 233 (2000) 19–40.

[21] I.K. Oh, I. Lee, Thermal snapping and vibration characteristics of cylindrical composite panels using layerwise theory, *Composite Structures* 51 (2001) 49–61.
[22] K.M. Liew, J. Yang, S. Kitipornchai, Postbuckling of piezoelectric FGM plates subject to thermo-electro-mechanical loading, *International Journal of Solids Structures* 51 (2003) 3869–3892.
[23] J. Yang, S. Kitipornchai, K.M. Liew, Large amplitude vibration of thermo-electro-mechanically stressed FGM laminated plates, *Computer Methods in Applied Mechanics and Engineering* 192 (2003) 3861–3885.
[24] J.N. Reddy, A simple higher-order theory for laminated composite plates, *Journal of Applied Mechanics* 51 (1984) 745–752.
[25] D.O. Brush, B.O. Almroth, *Buckling of Beams, Plates and Shells*, McGraw-Hill, New York, 1975.
[26] W. Han, M. Petyt, Geometrically nonlinear vibration analysis of thin, rectangular plates using the hierarchical finite element method-I: The fundamental mode of isotropic plates, *Computers and Structures* 63 (1997) 295–308.
[27] Y. Shi, R.Y.Y. Lee, C. Mei, Thermal postbuckling analysis of composite plates using the finite element modal coordinate method, *Journal of Thermal Stresses* 22 (1999) 595–614.